https://doi.org/10.37434/tpwj2020.08.06

PEQULIARITIES OF FORMATION OF DISSIMILAR NICKEL-BASE ALLOY JOINTS IN FRICTION WELDING

I.V. Ziakhor, M.S. Zavertannyi, A.M. Levchuk and **L.M. Kapitanchuk**
E.O. Paton Electric Welding Institute of the NAS of Ukraine
11 Kazymyr Malevych Str., 03150, Kyiv, Ukraine. E-mail: office@paton.kiev.ua

When creating new designs of aircraft gas turbine engines, the urgent task is to replace the mechanical fasteners of structural elements from high-temperature nickel alloys with welded joints. The paper presents the results of research on the processes of heating, deformation and formation of the structure of joints during friction welding (FW) of dissimilar alloys — granular alloy EP741NP with wrought alloy EI698VD and casting alloy VZhL12U. The minimum values of pressure, at which upsetting is provided (deformation of billets in macrovolumes) are determined. The critical value of pressure, exceeding which leads to a change in the nature of the upsetting process in friction welding of EP741NP and VZhL12U alloys — from uniform shortening of the billets to stepwise. The range of changes in technological parameters of friction welding process, which ensures formation of defect-free welded joints, is determined. Microhardness studies have shown absence of areas with reduced microhardness in the zone of the joint of EP741NP and VZhL12U alloys. 22 Ref., 2 Tables, 11 Figures.

Keywords: friction welding, high-temperature nickel-base alloys, deformation, γ′-phase

High-temperature nickel alloys (HTNA): wrought, granular and casting, are widely used in manufacture of discs and blades of aviation gas turbine engines (GTE) [1–3]. Because of nonuniform heating and loading, turbine elements are made from dissimilar HTNA, which are connected by mechanical fasteners, that leads to greater weight of the turbine and engine as a whole. When new designs of aviation GTE are developed, replaced of mechanical fasteners by welded joints will allow reducing the engine weight at preservation of other service properties [4–8]. Therefore, application of welded assemblies from dissimilar HTNA in promising structures of aviation GTE is an extremely urgent problem.

Methods of fusion welding [9, 10], brazing [11, 12], and friction welding [13–18] are used to produce HTNA permanent joints. HTNA multicomponent alloying can result in formation of eutectic interlayers and chemical element segregation in brazing that adversely affects the characteristics of joint high-temperature resistance. Sound (defectfree) joints of HTNA are produced by fusion welding processes at the total content of aluminium and titanium (main elements forming the strengthening γ′-phase) in the alloy, which is not higher than 4 wt.%. At higher alloying of the alloys, the welds are prone to cracking [19].

Friction welding (FW) of different technological modifications — rotational FW and linear FW, is becoming ever wider applied abroad for producing permanent joints of high-alloyed HTNA, [13–15].

Producing sound joints of HTNA at FW is possible under the condition of providing a certain level of heat generation power during heating and pressure sufficient for metal deformation in the joint zone to a specified extent. Heat generation power value at FW is determined by a combination of relative rotation speed (or frequency and amplitude of relative vibration displacement at linear FW), pressure at heating and friction coefficient of specific alloys. It is known that sound joints cannot be produced without plastic deformation of metal macrovolumes in the zone of billet contact at FW [20]. Temperature range of deformation (TRD) of the high-temperature alloy depends on its chemical composition and is limited, on the one hand by the temperatures of recrystallization T_{recr} and complete dissolution of strengthening γ′-phase, T_{solvus}, and on the other hand — by the melting point — $T_{solidus}$.

With increase of the degree of HTNA alloying (Table 1) and volume fraction of γ′-phase, the alloy TRD becomes narrower — alloy melting point decreases, and the values of T_{recr} and T_{solvus} temperatures, rise. As producing a sound joint requires providing a certain extent of deformation of one or both of the billets, at which the oxides and the adsorbed films are pressed out beyond the cross-section limits [20], the value of billet upsetting is one of the parameters, controlled at

I.V. Ziakhor — https://orcid.org/0000-0001-7780-0688, M.S. Zavertannyi — https://orcid.org/0000-0002-8415-8555
A.M. Levchuk — A.M. https://orcid.org/0000-0002-0361-7394

© I.V. Ziakhor, M.S. Zavertannyi, A.M. Levchuk and L.M. Kapitanchuk, 2020

Table 1. Chemical composition of studied alloys, wt.%

Alloy	Ni	Cr	Ti	Al	W	Mo	Nb	Co	V	Mn	Si	Hf	C
EI698VD	Base	14.4	2.74	1.69	0.05	2.98	2.04	–	0.05	0.08	0.20	–	0.05
VZhL12U	Same	9.7	4.5	5.4	1.4	3.1	0.8	14.0	0.8	0.01	0.03	–	0.18
EP741NP	»	9	1.9	5.1	5.6	3.8	2.6	15.8	–	0.5	0.5	0.3	0.04

Table 2 Some phase characteristics of studied alloys [21, 22]

Alloy	Total amount of γ′-phase, %	Solidus temperature, $T_{solidus}$	Temperature limit of γ′-phase dissolution, T_{solvus}, °C	Recrystallization temperature, $T_{recr.}$, °C	Deformation temperature		Hot plastic deformation ability
					Start	End	
EI698VD	25.0	1320	1030	1050–1100	1160	1000	Good
EP741NP	60.0	1270	1190	1150–1170	1140	1030	Very poor
VZhL12U	65.0	1273	1220	–	–	–	Same

FW. Sound joints can be formed only when a certain upsetting value has been reached [13, 17, 20].

Studying the thermal cycles and process of deformation (upsetting) of the billets at FW of dissimilar HTNA, in particular, disc (wrought and granular) and blade (casting) alloys, which are used in the design of turbines of local GTE developers and manufacturers, is of scientific interest and practical value.

The objective of the work is to establish the peculiarities of heating and deformation of dissimilar HTNA, formation of joint microstructure, depending on values of FW mode parameters, and on this base improve FW technology, which will ensure formation of sound welded joints.

Experimental procedure. Processes of heating and deformation at FW of dissimilar commercial alloys were studied: casting alloy VZh12U, granular alloy EP741NP, wrought alloy E1698VD, which are used in the designs of local developers and manufacturers of aviation GTE: SC «Ivchenko-Progress», JSC «Motor Sich». Specifically, as regards «disc–disc» welded assembly, FW of dissimilar nickel alloys — wrought E1698VD with granulated EP741NP, and for «disc–blade» assembly — granular EP741NP with casting VZhL12U, were studied.

Investigations were conducted on cylindrical samples of 12–15 mm diameter. Chemical composition and some characteristics of the studied alloys are given in Table 1 and Table 2.

Before welding, heat treatment of HTNA was performed by the following mode:

- for EI698VD alloy: first quenching at 1100 °C, soaking for 8 h; second quenching at 1000 °C, 4 h, ageing at 775 °C, 16 h;
- for EP741NP alloy: 1210 °C, soaking for 8 h, 870 °C, 32 h;
- for VZhL12U alloy: 1210 °C, soaking for 4 h; 950 °C, 16 h, and cooling in air in all the cases.

Test welding was conducted in laboratory unit ST120 with spindle rotation drive based on a dc motor with regulated rotation frequency in 40–300 rad/s range. Hydraulic drive ensures three-stage cyclogram of axial force application: rubbing-heating-forging in the range of 5–120 kN. ST120 unit allows realization of the technology of combined FW with regulated deceleration of rotation (Figure 1). During experiments on FW of EI698VD and EP741NP alloys, the process parameters were set in the following ranges: peripheral speed V = 1.0–1.5 m/s, heating pressure P_h = 50–440 MPa. In FW of EP741NP and VZhL12U alloys heating pressure was varied in the range of P_h = = 100–550 MPa, at peripheral speed V = 1 m/s.

Recording of welding mode parameters was performed by PC-based operational system using pressure sensor ADZ-SML-20.0-1, and upset control sensor SR 18-25-S «Megatron». During FW, recording of thermal cycles was performed, using chromel-alumel thermocouples of 0.5 mm diameter, welded to the billet surface at a certain distance from the contact zone. Measurement results were used to determine the distribution of sample heating temperature along the axis for different values of heating time t_h. Temperature values in the contact zone were found by interpolation of experimental data by the exponential law.

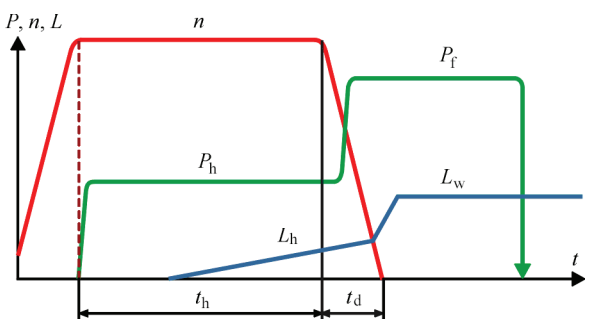

Figure 1. Cyclogram of combined FW with regulated deceleration of rotation: n — rotation frequency; P_h, P_f — pressure at heating and forging; L — upsetting; t_h — heating time; t_d — time of rotation deceleration

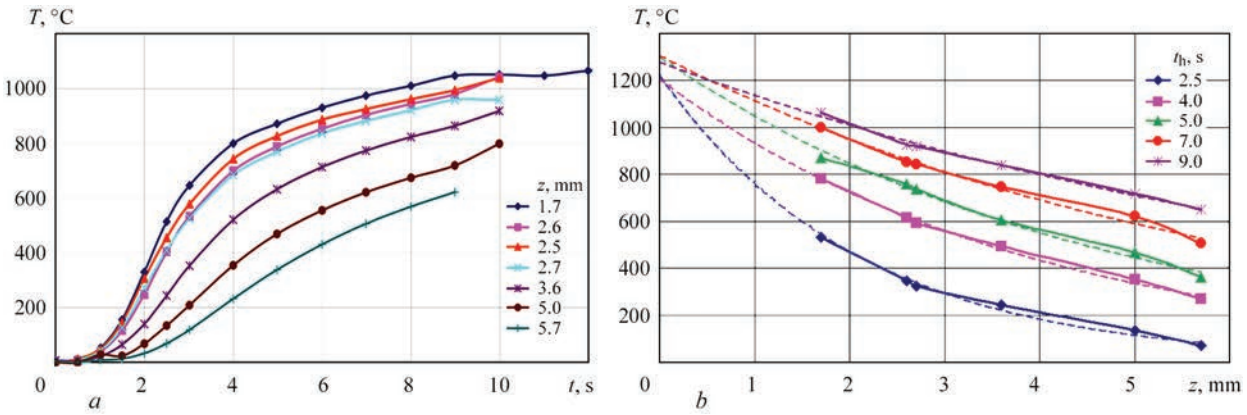

Figure 2. Change in time of temperature on the surface of a sample of EP741NP alloy at the distance from the contact surface z = 1.7; 2.6; 2.5; 2.7; 3.6; 5.0; 5.7 mm (*a*); temperature distribution at different values of heating time t_h = 2.5; 4.0; 5.0; 7.0; 9.0 s (*b*)

Tensile mechanical testing of standard samples of welded joints (GOST 1497–84) was conducted in TsDM-10 machine. Presence of surface defects (cracks, delamination) in the joint zone was detected at visual examination of the joint surface at x10 magnification, as well as using MMP4 microscope. Welded joint geometry and presence of defects were determined by metallographic examination of microsections prepared by a standard procedure.

Microstructure was studied in a light microscope Neophot-32, scanning electron microscope (SEM) JSM-35SA, Auger-microprobe JAMP-9500F, JEOL. Element distribution in the joint zone was determined using EDS-analyzer «INCA-450», Oxford Instruments Company, with approximately 1 μm diameter of the probe. Optical and electron microscopy was performed on microsections, prepared using chemical and electrolytic methods of structure detection. Measurements of metal microhardness in the HAZ across the joint line in 50 μm steps were conducted in microhardness meter M-400 (LECO) at 1.0–5.0 N load.

Experimental results. Results of studying the thermal cycles at different distance from the contact zone z at FW of EP174NP alloy to EI698VD alloy are given in Figure 2, *a* (peripheral speed V = 1.2 m/s, heating pressure P_h = 300 MPa). Obtained data were used to establish the temperature distribution from the side of EP741NP alloy for the moments of heating time t_h = 2.5; 4; 5; 7; 9 s (Figure 2, *b* — solid lines). Interpolation of experimental data to the contact plane (z = 0 mm) revealed that the temperature in the contact zone (Figure 2, *b* — dashed lines) is higher than melting temperature $T_{solidus}$ of EP741NP alloy.

Thermal cycles at different distance from contact zone z at FW of EP741NP alloy with VZhL12U alloy are given in Figure 3, *a* (V = m/s, P_h = 150 MPa), temperature distribution at different values of heating time t_h = 10, 15, 20, 25 s is shown in Figure 3, *b*).

It is established that the rate of metal heating in the contact zone at the initial stage of WF process reaches 1000 °C/s that in combination with exceeding the solidus temperature of EP741NP alloy can lead to partial melting of grain boundaries from the side of this alloy, and formation of a solid-liquid interlayer in the joint zone. Analysis of the temperature fields shows exceeding T_{solvus} and T_{recr} temperature in the contact zone for all the studied alloys. The width of the heating zone of high alloys EP741NP and VZhL12U up to the temperature higher than the values of temperatures of recrystallization and complete dissolution of strength-

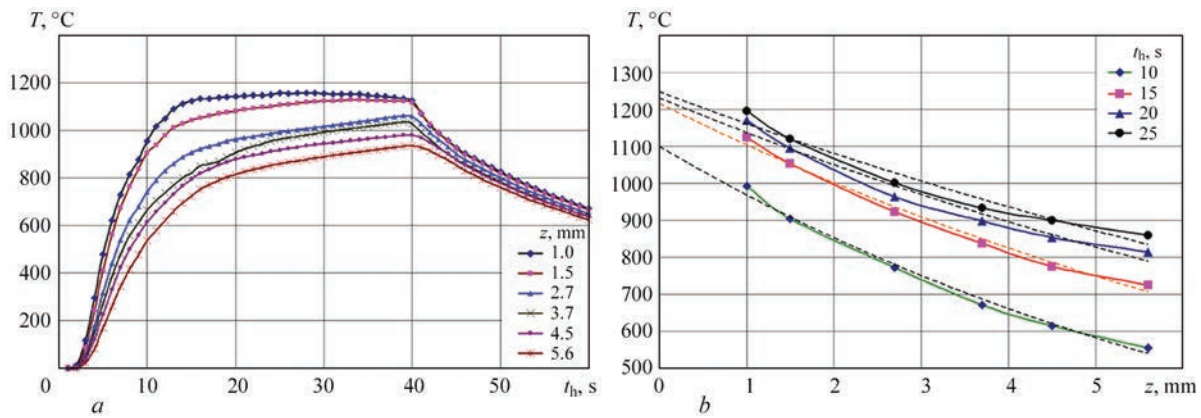

Figure 3. Change in time of temperature on the surface of a sample of VZhL12U alloy at FW with EP1741NP alloy at the distance from contact surface z = 1.0; 1.5; 2.7; 3.7; 4.5; 5.6 mm (*a*); temperature distribution from the side of VZhL12U alloy at different values of heating time t_h = 10; 15; 20; 25 s (*b*)

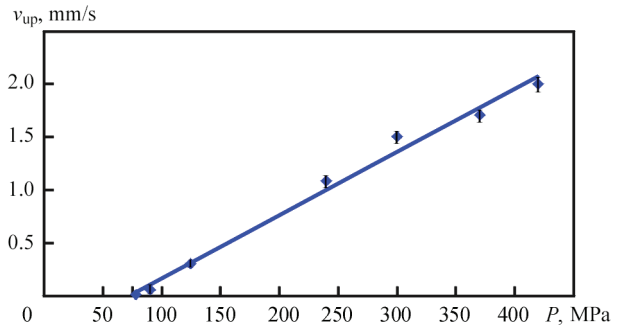

Figure 4. Dependence of upsetting speed on pressure at FW of EP1741NP alloy to EI698VD alloy (V = 1.0 m/s)

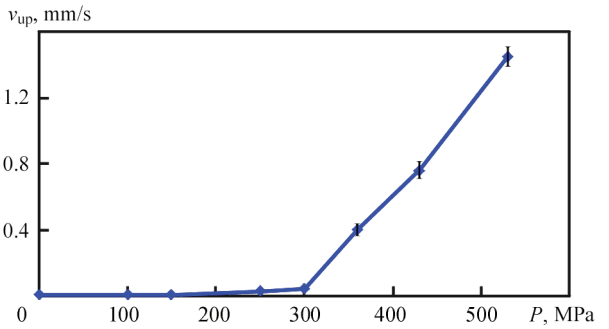

Figure 5. Dependence of upsetting speed on pressure at FW of EP1741NP and VZhL12U alloys (v = 1.0 m/s)

ening γ′-phase, is equal to less than 1 mm, that largely determines the conditions of billet deformation.

Deformation of billets (upsetting process) was studied at formation of welded joints of EI698VD alloy with EP741NP alloy and of VZhL12U alloy with EP741NP alloy. It is found that in the first case upsetting occurs predominantly due to wrought EI698VD alloy. Value of shortening of the billet from granular EP741NP alloy does not exceed 20 % of the total upset value at FW. Experimental results were used to plot the dependence of upsetting speed in FW of EI698VD alloy with EP741NP alloy on welding pressure (Figure 4). Dependence can be expressed by a linear function, in which upsetting speed rises in proportion to increase of welding pressure. As one can see from Figure 4, the process of billet upsetting begins, when pressure value $P_{h.min}$ = 80 MPa is exceeded.

Figure 5 gives the results of studying the upsetting process at FW of granular alloy EP741NP with casting alloy VZhL12U. It is established that at peripheral speed V = 1 m/s the process of billet upsetting at pressure value below $P_{h.min}$ = 300 MPa is practically not observed. Only after this value has been exceeded, the upsetting begins, which is accompanied by billet deformation in macrovolumes. In the range of pressure values of 300–530 MPa, the dependence of upsetting speed on pressure can be approximated by a linear function.

Thus, the process of upsetting (billet shortening) at FW starts only at a certain minimum value of pressure at heating $P_{h.min}$, which is different for a specific combination of alloys being welded. In welding of EI698VD and EP741NP alloys, welding starts in the case of exceeding pressure value $P_{h.min} > 80$ MPa and for a combination of VZhL12U and EP741NP alloys — at exceeding of pressure $P_{h.min}$ = 300 MPa. At smaller pressure values, metal heating in the contact zone up to solidus temperature of both or one of the alloys and formation of a thin metal interlayer in the solid-liquid state takes place. However, no upsetting of the billets, accompanied by ousting the oxides and adsorbed films beyond the billet cross-section limits, is observed. Under these conditions, sound welded joints cannot be formed.

Figure 6 gives the data on recording the parameters of the process of FW of EP741NP alloy with VZhL12U alloy. Anomalous step nature of the upsetting process at exceeding a certain critical value of pressure P_{crit} was found. Such a nature of the upsetting process is not characteristic for FW of other combinations of metals and alloys that were studied by the authors.

In particular, for peripheral speed of 1 m/s, P_{crit} value is equal to P_{crit} = 550 MPa. Billet deformation from the side of EP741NP alloy at P_h = 550 MPa is characterized by alternate change of the shortening rate: areas with a low upsetting speed v_{up} = 0.4–0.8 mm/s change to jumplike high-speed upsetting (v_{up} = 5 mm/s). Here, in areas with higher upsetting speed emissions of heated particles of metal, which probably was in the solid-liquid state, from the contact zone, were observed.

Obtained data were the base for determination of the change of technological parameters of FW process of dissimilar HTNA, namely granular alloy EP741NP with wrought disc alloy EI698VD and casting blade alloy VZhL12U. Technology of combined FW was improved. It ensures absence of anomalous phenomena in the upsetting process and formation of sound joints at FW of dissimilar high HTNA.

A photo of macrosection of the joint of VZhL12U and EP741NP alloys, produced by the improved technology of combined FW, is given in Figure 7, *a*. In the

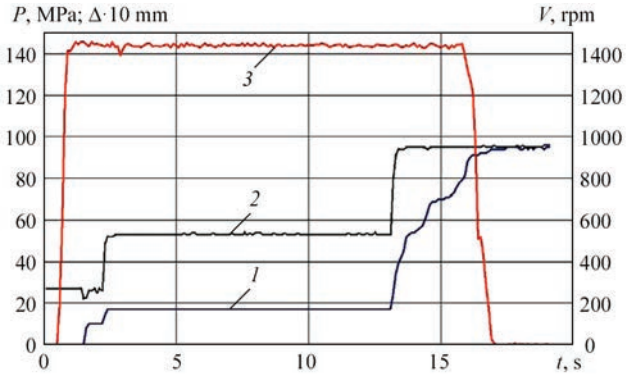

Figure 6. Results of recording the parameters of FW of VZhL12U and EP1741NP alloys: *1* — welding pressure P; *2* — upsetting (shortening) of the billet Δ; *3* — rotation frequency n

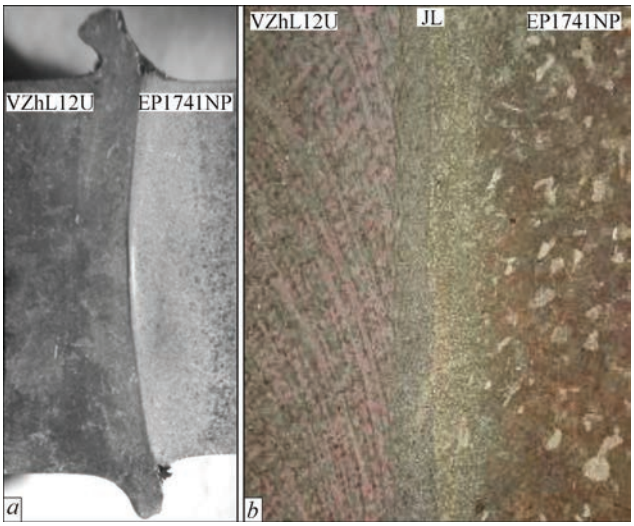

Figure 7. Macrosection (×100) (*a*) and microstructure (*b*) of the joint of VZhL12U and EP1741NP alloys

joint zone, formation of a reinforcement characteristic for FW from the side of VZhL12U alloy and its absence from the side of EP741NP alloy, are observed. Any defects, in particular, cracks and undercuts in the peripheral part of the billet cross-section are absent in the joint zone (Figure 7, *b*).

Microstructure (Figure 8) of the welded joint from the side of both the alloys is characterized by presence of typical for FW areas, located on both sides from the joint line (JL): zones of dynamic recrystallization (ZDR1 and ZDR2); zones of thermomechanical impact

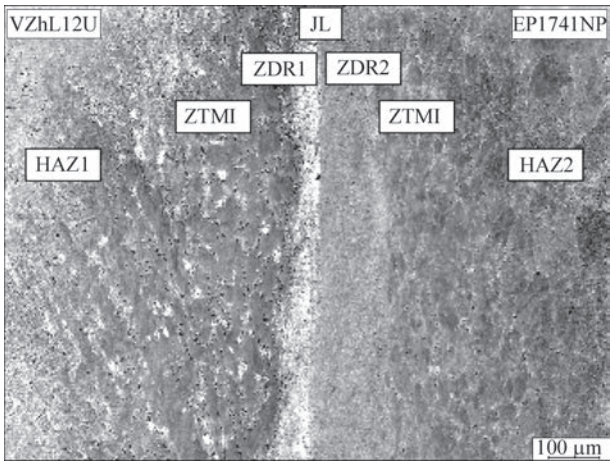

Figure 8. SEM image of the zone of VZhL12U and EP1741NP alloys joint

(ZTMI1 and ZTMI2), and heat-affected zones (HAZ1 and HAZ2), respectively, for VZhL12U and EP741NP. ZTMI1 structure from the side of VZhL12U alloy is characterized by the change of orientation of base metal dendrites in the radial direction that is indicative of plastic deformation of this alloy in the macrovolumes.

Figure 9 gives the microstructure of metal on the line of the joint of VZhL12U and EP741NP alloys. In different parts of billet cross-section (central, peripheral) similarity of metal microstructure along the JL is observed. Average grain size in the zone of dynamic recrystallization of the alloys is equal to 3–4 μm from the side of EP741NP alloy and is close to 2 μm from the side of

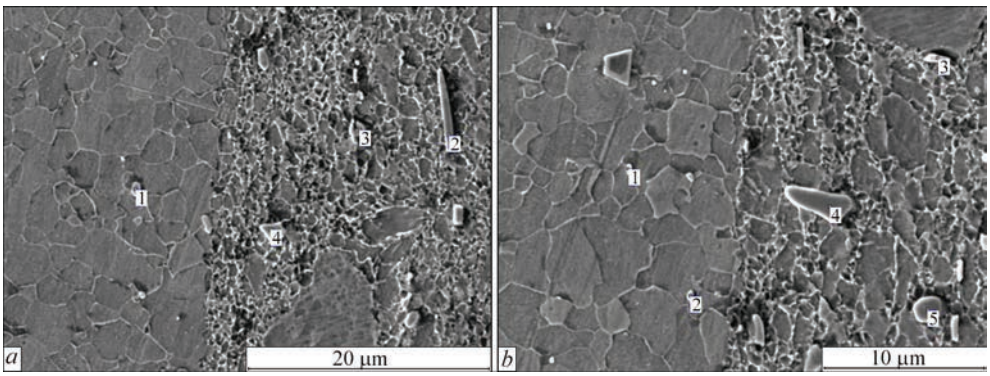

Figure 9. SEM image of microstructure of the zone of VZhL12U and EP1741NP alloys joint in the central (*a*) and peripheral (*b*) parts of billet cross-section

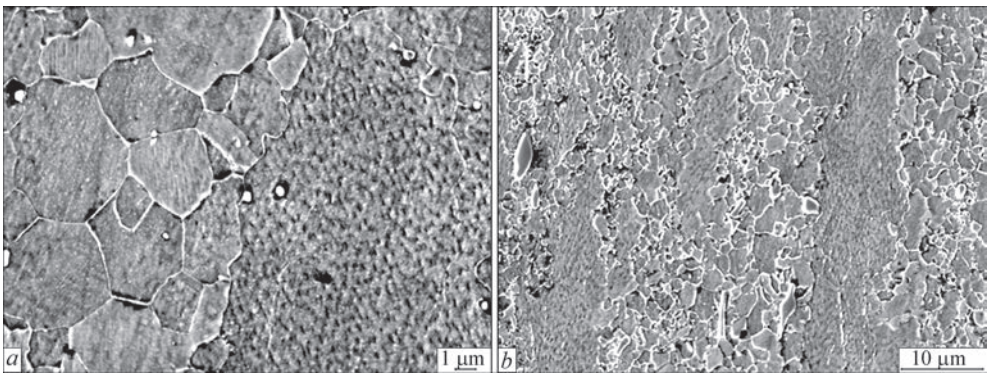

Figure 10. SEM image of the boundary between ZDR and ZTMI of EP1741NP (*a*), and VZhL12U (*b*) alloys

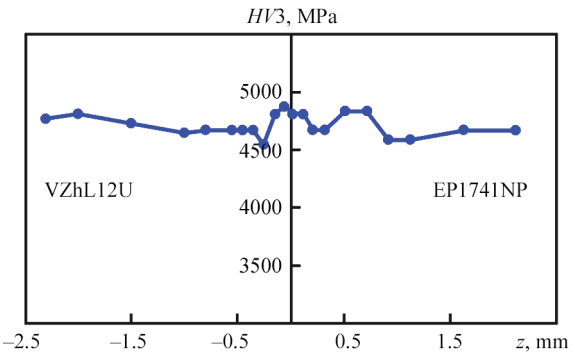

Figure 11. Microhardness distribution in the zone of VZhL12U and EP1741NP alloys joint

VZhL12U alloy. Metal microstructure along JL is indicative of solid-phase nature of joint formation, both in the central, and in the peripheral parts of billet cross-section.

When studying metal microstructure in ZTMI (Figure 10, *a*), a clear-cut boundary between ZDR and ZTMI is observed from the side of EP741NP — fine dynamically recrystallized ZDR grains, where during FW strengthening γ′-phase was completely dissolved (on the left), and partially deformed grain in ZTMI with partially dissolved γ′-phase (on the right). Microstructure of ZMTI of VZhL12U alloy is characterized by presence of base metal grains deformed during FW (Figure 10, *b*), in which strengthening γ′-phase is partially dissolved, and of dynamically recrystallized grains of up to 3 μm size, where γ′-phase is completely dissolved.

Figure 11 gives microhardness distribution in the zone of welded joint of EP741NP and VZhL12U alloys. Absence of areas with lower microhardness values was established. Microhardness increase near the joint line was detected, which, most probably, is related to grain refinement in the dynamic recrystallization zone.

Conclusions

1. Investigations of thermal cycles in friction welding of dissimilar high-temperature nickel alloys EP741NP and EI698VD, as well as EP741NP and VZhL12U alloys showed the possibility of achieving in the contact zone the solidus temperature of one of the alloys and formation of an interlayer in the solid-liquid state.

2. Investigations of the process of deformation of EP741NP with EI698VD, and VZhL12U alloys at FW with peripheral speed V = 1.0–1.2 m/s allowed establishing minimum values of pressure $P_{h.min}$, at which upsetting (deformation in macrovolumes) of the billets is ensured: $P_{h.min}$ = 80 MPa for a combination of EP741NP with EI698VD and $P_{h.min}$ = 300 MPa for a combination of EP741NP and VZhL12U.

3. Anomalous step nature of upsetting at FW of EP741NP and VZhL12U alloys at exceeding a certain critical value of pressure P_{crit} was detected. In particular, for peripheral speed V = 1 m/s this value is P_{crit} = 550 MPa. An optimum range of the change of technological parameters of FW process of dissimilar HTNA was determined, namely granular alloy EP741NP with wrought disc alloy EI698VD and casting blade alloy VZhL12U.

4. Technology of combined FW was improved, which provides absence of anomalous phenomena in upsetting process and formation of sound joints at FW of dissimilar high HTNA. Investigations of microhardness distribution in the joint zone of EP741NP and VZhL12U alloys showed absence of areas with lowered microhardness values.

1. Furrer, D., Fecht, H. (1999) Ni-based superalloys for turbine discs. *JOM*, **1**, 14–17.
2. Das, N. (2010) Advances in nickel-based cast superalloys. *Transact. of the Indian Institute of Metals,* 63(**2–3**), 265–274.
3. Romanov, V.V., Koval, V.A. (2020) Application of new materials in conversion of ship and aviation GTE into stationary GTI. *Eastern-European J. of Enterprise Technologies*, **3**, 4–7 [in Russian].
4. Maslenkov, S.B. (2001) *Technology of producing of permanent joint in manufacture of gas turbine engines.* Moscow, Nauka i Tekhnologii [in Russian].
5. Ospennikova, O.G., Lukin, V.I., Afanasiev-Khodykin, A.N., Galushka, I.A. (2018) Manufacture of «blisk» type structure of dissimilar material combination (Review). *Trudy VIAM,* **10**, 10–16. DOI: 10.18577/2307-6046-2018-0-10-10-16 [in Russian].
6. Magerramova, L.A. (2011) Application of bimetal blisks, manufactured by HIP method from granulated and cast nickel superalloys to improve reliability and service life of gas turbines. *Vestnik UGATU*, 15(**4**), 44, 33–38 [in Russian].
7. Ospennikova, O.G. (2012) Strategy of development of heat-resistant alloys and steels of special purpose, protective and thermal-barrier coatings. *Aviats. Materialy i Tekhnologii*, **5**, 19–36 [in Russian].
8. Shmotin, Yu.N., Starkov, R.Yu., Danilov, D.V. et al. (2012) New materials for advanced engine of PJSC NPO Saturn. *Ibid*., **2**, 6–8 [in Russian].
9. Lukin, V.I., Kovalchuk, V.G., Golev, E.V. et al. (2016) Electron beam welding of high-strength cast nickel alloy VZh172L. *Svarochn. Proizvodstvo*, **5**, 44–49 [in Russian].
10. Yushchenko, K.A., Zadery, V.A., Zvyagintseva, A.V. et al. (2008) Sensitivity to cracking and structural changes in EBW of single crystals of heat-resistant nickel alloys. *The Paton Welding J.*, **2**, 6–13.
11. Rylnikov, V.S., Afanasiev-Khodykin, A.N., Timofeeva, O.B. (2013) Features of technology of diffusion brazing of heat-resistant alloy EP975 and cast single-crystal intermetallic alloy VKNA-4U for blisk structure. *Svarochn. Proizvodstvo*, **7**, 19–25 [in Russian].
12. Rylnikov, V.S., Afanasiev-Khodykin, A.N., Galushka, I.A. (2013) Technology of brazing of «blisk» type structure from dissimilar alloys. *Trudy VIAM*, **10**. URL: http://viam-works.ru/plugins/content/journal/uploads/articles/pdf/251.pdf [in Russian].
13. Li, W., Vairis, A., Preuss, M., Ma, T. (2016) Linear and rotary friction welding review. *Int. Materials Reviews*, 61(**2**), 71–100. DOI: 10.1080/09506608.2015.1109214.
14. Senkov, O.N., Mahaffey, D.W., Semiatin, S.L., Woodward, C. (2014) Inertia friction welding of dissimilar superalloys Mar-M247 and LSHR. *Metallurgical and Materials Transact. A*, **45A**, 5545–5561. DOI: 10.1007/s11661-014-2512-x.

15. Ola, O.T., Ojo, O.A., Wanjara, P., Chaturvedi, M.C. (2011) Analysis of microstructural changes induced by linear friction welding in a nickel-base superalloy. *Ib d.*, **2** , 3761–3777. DOI: 10.1007/s11661-011-0774-0.
16. Lukin, V.I., Samorukov, M.L. (2017) Peculiarities of formation of structure of heat-resistant wrought alloy VZh175 welded joints, produced by rotary friction welding. *Sva och Proizvodstvo*, **6**, 25–33 [in Russian].
17. Bychkov, V.M., Selivanov, A.S., Medvedev, A.Yu. et al. (2012) Investigation of weldability of heat-resistant nickel alloy EP742 by linear friction welding method. *Vestn k UGATU*, 16(**7**), 52, 112–116 [in Russian].
18. Lukin, V.I., Kovalchuk, V.G., Samorukov, M.L. et al. (2010) Peculiarities of friction welding technology of joints from VKNA-25 and EP975 alloys. *Sva och Proizvodstvo*, **5**, 28–33 [in Russian].
19. Sorokin, L.I. (2005) Formation of hot cracks in welding of heat-resistant nickel alloys (Review). *Ibid.*, **7**, 29–33 [in Russian].
20. Lebedev, V.K., Chernenko, I.A., Villya, V.I. (1987) *Friction weldig* : Refer. Book. Leningrad, Mashinostroenie [in Russian].
21. Vaulin, D.D., Eremenko, V.I., Vlasova, O.N. et al. (2006) Technological features of the manufacture of stamped semi-finished products from heat-resistant nickel alloys. In: *Persp ctive techl ogies for ligh d sp cil l loys*. Moscow, FIZMATLIT, 294–301 [in Russian].
22. Bondarev, B.I., Fatkullin, O.Kh., Eremenko, V.N. et al. (1999) Development of heat-resistant nickel alloys for gas turbine discs. *Tekhl ogiyL yogkikhSp u ov*, **3**, 49–53 [in Russian].

Received 13.07.2020